HOKKAIDO UNIVERSITY

Title	A study on the function of the phospholipid flippase Drs2 in the endocytic-recycling pathway
Author(s)	花松, 久寿
Degree Grantor	北海道大学
Degree Name	博士(生命科学)
Dissertation Number	甲第11409号
Issue Date	2014-03-25
DOI	https://doi.org/10.14943/doctoral.k11409
Doc URL	https://hdl.handle.net/2115/55776
Type	doctoral thesis
File Information	Hisatoshi_Hanamatsu.pdf

Hokkaido University Collection of Scholarly and Academic Papers : HUSCAP

A study on the function of the phospholipid flippase Drs2 in the endocytic-recycling pathway.

A DISSERTATION

submitted to the Graduate School of Life Science,

Hokkaido University

in partial fulfillment of the requirements for the degree

DOCTOR OF LIFE SCIENCE

by

Hisatoshi Hanamatsu

2014

CONTENTS

ABSTRACT ····· 1

INTRODUCTION ····· 2

MATERIALS AND METHODS ····· 5

RESULTS ····· 10

DISCUSSION ····· 17

REFERENCES ····· 20

ACKNOWLEDGEMENTS ····· 24

TABLES ····· 25

FIGURES ····· 29

ABSTRACT

Phospholipid composition of biological membranes differs between the cytoplasmic and exoplasmic leaflets. The type 4 subfamily of P-type ATPases are phospholipid flippases that generate such membrane phospholipid asymmetry. Drs2p, a flippase in budding yeast, is involved in the endocytic recycling pathway. Drs2p is implicated in clathrin-coated vesicle formation, but the underlying mechanisms are not clearly understood. Here I show that the carboxyl-terminal cytoplasmic region of Drs2p directly binds to Rcy1p, an F-box protein that is also required for endocytic recycling. The Drs2p-binding region was mapped to the amino acids 574-778 region of Rcy1p, and a mutant Rcy1p lacking this region was defective in endocytic recycling of a v-SNARE Snc1p. I isolated Drs2p point mutants that reduced the interaction with Rcy1p. The mutation sites were clustered within a small region (amino acids 1260-1268) of Drs2p. Although these point mutants did not exhibit clear phenotypes, combination of them resulted in cold-sensitive growth, defects in endocytic recycling of Snc1p, and defective localization of Rcy1p to endosomal membranes like the *drs2* null mutant. These results suggest that the interaction of Drs2p with Rcy1p plays an important role for Drs2p function in the endocytic recycling pathway.

INTRODUCTION

The type 4 subfamily of P-type ATPases (P4-ATPases) are phospholipid flippases that transport specific phospholipids from the exoplasmic to cytoplasmic leaflet of membranes to generate and maintain asymmetrical distribution of phospholipids (*1-3*). In *Saccharomyces cerevisiae*, there are five members of this subfamily, Drs2p, Dnf1p, Dnf2p, Dnf3p, and Neo1p. Of these, Drs2p, Dnf1p and Dnf2p, and Dnf3p form a complex with Cdc50 family non-catalytic subunits, Cdc50p, Lem3p, and Crf1p, respectively (**Fig. 1**), for their exit out of the endoplasmic reticulum (ER) and proper localization (*4,5*). Cdc50p-Drs2p is localized to early endosomes and the *trans*-Golgi network (TGN) (*4,6-9*). One major function of Drs2p is to promote vesicle formation from early endosomes in the early endosome-to-TGN transport pathway or the endocytic recycling pathway. The exocytic vesicle-soluble N-ethylmaleimide-sensitive factor attachment protein receptor (v-SNARE) Snc1p, which is recycled from the plasma membrane via early endosomes to the TGN, accumulated intracellularly in the *drs2*Δ mutant (**Fig. 2**) (*4,7*). This defect was most severe in the *cdc50*Δ *lem3*Δ *crf1*Δ mutant (equivalent to the *drs2*Δ *dnf1*Δ *dnf2*Δ *dnf3*Δ mutant) in which GFP-Snc1p was trapped in massively accumulated large early endosome-derived structures (*5*).

The *drs2*Δ mutant exhibits TGN defects comparable with those exhibited by strains with clathrin mutations and is actually defective in the formation of clathrin-coated vesicles (CCVs) (*6*). Thus, Drs2p may be involved in forming a CCV on early endosomal membranes. Because clathrin has no intrinsic lipid-binding ability, it is linked to membranes by adaptors, which bind to lipids and/or the cytoplasmic domains of cargo proteins (*10*).

The AP-1 clathrin adaptor has been shown to be involved in both anterograde and retrograde transport between early endosomes and the TGN in yeast (*11-13*). Genetic studies suggested that Cdc50p-Drs2p and AP-1 could function in the same pathway: both a mutation in AP-1 and the *cdc50*Δ/*drs2*Δ mutation exhibited synthetic growth defects with *gcs1*Δ (Arf GAP) and *gga1*Δ *gga2*Δ (monomeric clathrin adaptors) mutations, but the *ap-1 cdc50*Δ/*drs2*Δ mutant did not exhibit a synthetic defect (*13,14*).

Rcy1p, an F-box protein, was also identified as a factor involved in the endocytic recycling pathway (*15-17*). The F-box proteins were first described as components of the Skp1-Cullin-F-box protein (SCF) ubiquitin-ligase E3 complex catalyzing the ubiquitination of proteins, and are thought to provide substrate specificity to the complex (*18,19*). Although Rcy1p was reconstituted with the other subunits to form a complete SCF complex *in vitro* (*20*), it remains unknown whether Rcy1p functions as a subunit of a ubiquitin ligase *in vivo* (*16*). Furuta *et al*. demonstrated a close functional relationship between Rcy1p and Cdc50p-Drs2p in the endocytic recycling pathway (*5*): (i) in addition to phenotypic similarity, both *rcy1*Δ and *drs2*Δ mutations exhibited the same array of synthetic lethal interactions with mutations in endocytosis- and recycling-related genes; (ii) the *cdc50*Δ *rcy1*Δ mutant did not show a synthetic growth defect; and (iii) Rcy1p was coimmunoprecipitated with Cdc50p-Drs2p. Thus, Drs2p and Rcy1p may function in the same pathway in which Rcy1p plays a key role when Drs2p promotes CCV formation by flipping phospholipids. However, it has not been demonstrated that the interaction with Rcy1p is crucial for the Drs2p function.

Here I demonstrate that Drs2p directly interacts with Rcy1p via its

carboxyl-terminal (C-terminal) region. Analysis of Drs2p mutants that are defective in the interaction with Rcy1p indicates that the interaction with Rcy1p is important for the Drs2p function in the early endosome-to-TGN transport. Rcy1p might function as an adaptor that facilitates CCV formation at the site where Drs2p flips phospholipids.

Abbreviations: Arf, ADP ribosylation factor; Arl, ADP-ribosylation factor- like; 3-AT, 3-aminotriazole; CCV, clathrin-coated vesicle; C-terminal, carboxyl-terminal; DIC, differential interference contrast; ER, endoplasmic reticulum; IPTG, isopropyl- β -D-1-thiogalactopyranoside; MBP, maltose binding protein; mRFP1, monomeric red fluorescent protein 1; N-terminal, amino-terminal; SCF, Skp1-Cullin-F-box protein; SDS-PAGE, sodium dodecyl sulfate-poly acrylamide gel electrophoresis; TGN, trans-Golgi network; v-SNARE, vesicle-soluble N-ethylmaleimide-sensitive factor attachment protein receptor; PBS, phosphate buffered saline; PMSF, phenylmethylsulfonyl fluoride

MATERIALS AND METHODS

Media and genetic techniques

Unless otherwise specified, strains were grown in rich medium (YPDA: 1% Bacto yeast extract [Difco, Detroit, MI], 2% Bacto peptone [Difco], 2% glucose, and 0.01% adenine). Strains carrying plasmids were selected in synthetic medium (SD) containing the required nutritional supplements (*21*). Standard genetic manipulations of yeast were performed as described previously (*22*). Yeast transformations were performed by the lithium acetate method (*23,24*). *Escherichia coli* strains DH5α and XL1-Blue were used for construction and amplification of plasmids and expression of GST- or maltose binding protein (MBP)-tagged proteins.

Strains and plasmids

Yeast strains used in this study are listed in Table I. Complete gene deletion (*DRS2* and *RCY1*) with *KanMX4* on Tanaka laboratory's strain background was performed using PCR fragments amplified from deletion strains as described (*4,5*). All constructs produced by the PCR-based procedure were verified by colony-PCR amplification to confirm the replacement occurred at the expected loci. The *rcy1*Δ*::hphMX4* strain (YKT1096) was constructed by replacing the *KanMX4* cassette of *rcy1*Δ*::KanMX4* with the *hphMX4* cassette from pAG32 (*25*). The *LEU2::mRFP1-SNC1* strain (YKT1778) was constructed by integrating the linearized pRS305-*mRFP1-SNC1* into the *LEU2* locus. The *rcy1*Δ *mRFP1-SNC1* strain (YKT1780) was constructed by a cross between YKT1096 and YKT1778 followed by tetrad dissection. Plasmids used in this study are listed in Table II.

Schemes detailing the construction of plasmids and sequences of PCR primers are available upon request.

Two-hybrid analysis

Two-hybrid assay was performed using strain L40 containing the LexA DNA-binding domain fusion plasmid and the GAL4 transcriptional activation domain fusion plasmid (*26*). The extent of the two-hybrid interaction was assayed by growth on SD-Trp-Leu-His plates supplemented with 5 mM of 3-aminotriazole (3-AT) (*27*). In the *LexA-RCY1* fusion plasmids, the C-terminal CAAX box motif for prenylation was deleted.

Reverse two-hybrid screening

The *DRS2(1216-1355)* gene was mutagenized by a PCR-based method as described previously (*28*). The *GAL4AD-2HA-DRS2(1216-1355)* fragment was amplified using primers GAL4-AD3 (5' GAATAATGAAATCACGGCTAG 3') and pGADC1-3' (5' GTAGACAAGCCGACAACC 3') and the plasmid pKT1865 (pGAD-C1-*2HA-DRS2(1216-1355)*) as a template. The resulting fragment and the linearized vector fragment prepared by digestion of pKT1865 with *Bam*HI and *Sal*I to eliminate *DRS2(1216-1355)* were simultaneously introduced into L40 containing pBTM116-*HA-RCY1*Δ*CAAX* (YHH22) to allow homologous recombination. Randomly selected 200 transformants grown on SD-Trp-Leu plates were replica-plated on SD-Trp-Leu-His + 3-AT plates, followed by incubation at 30°C for 2 days. Out of the 200 clones, 146 failed to grow, but it turned out by colony-PCR that only 26 clones contained

the structurally normal pKT1865. Of these 26 clones, 10 clones were confirmed to express the GAL4AD-2HA-Drs2(1216-1355) fusion protein of proper size by western blotting. The plasmids were recovered from these 10 clones, and the *drs2(1216-1355)* fragments were recloned into the pGAD-C1-*2HA* vector. The resulting plasmids were reintroduced into YHH22 to confirm the loss of the two-hybrid interaction. Finally, I obtained four mutant plasmids that weakly (M3 and M10) or strongly (M13 and M20) reduced the interaction with Rcy1p. Amino acid alterations in these mutants were determined by DNA sequencing.

Site-directed mutagenesis

Site-directed mutations were introduced into the *DRS2* C-terminal fragment by the overlap extension PCR method (*29*). pKT1865 and pKT1860 were used as templates to construct pGAD-C1 two-hybrid plasmids and Myc-tagged full-length-*DRS2* expression plasmids, respectively. The PCR products that contained desired mutations were digested with appropriate restriction enzymes, purified, and ligated into the original pKT1865 or pKT1860, which had been digested with the same restriction enzymes. The PCR-amplified region in each construct was sequenced to verify that only the desired substitution(s) was introduced.

Binding (pull-down) assay of MBP-Drs2p(1216-1355) with GST-Rcy1p(178-836)

GST-Rcy1p(178-836) and MBP-Drs2p(1216-1355) were expressed in DH5α with 100 μM isopropyl-β-D-1-thiogalactopyranoside (IPTG) for 7 h at 25°C and with 300 μM IPTG for 3 h at 30°C, respectively. The GST-Rcy1p(178-836)-expressing cells suspended in

phosphate buffered saline (PBS) with 1 mM phenylmethylsulfonyl fluoride (PMSF) were lysed by sonication using Bioruptor UCD-300 (Cosmo Bio, Tokyo, Japan) for 15 min at 30 s intervals and then by addition of Triton X-100 to a final concentration of 1% with gentle shaking. The crude lysate was centrifuged for 5 min at 20,000 x *g* to remove insoluble materials, and then GST-Rcy1p(178-836) was affinity-purified with glutathione-Sepharose 4B beads (GE Healthcare, Little Chalfont, Buckinghamshire, United Kingdom). The GST-Rcy1p(178-836)-bound beads, which were washed twice with PBS, were mixed with the cleared lysate of MBP-Drs2p(1216-1355) prepared as described above in Buffer A (20 mM Tris-HCl, pH 7.5, 200 mM NaCl, 1 mM EDTA, 1 mM PMSF). After rotating for 1 h at 4°C, the glutathione-Sepharose complex was pelleted, washed five times with wash buffer (PBS containing 1% Triton X-100, 200 mM NaCl), and then subjected to sodium dodecyl sulfate-poly-acrylamide gel Electrophoresis (SDS-PAGE), followed by western blotting using anti-GST and -MBP antibodies.

Immunoprecipitation and western blotting

Coimmunoprecipitation of HA-Rcy1p with Drs2p-Myc mutant proteins was performed as described previously (*5*). For SDS-PAGE of Drs2p-Myc, samples were heated at 37°C for 30 min before loading. Western blotting was performed as described previously (*9*). Anti-Myc, -HA, and -GST antibodies were used at a 1:1000 dilution, whereas anti-MBP antibodies were used at a 1:10000 dilution. The rabbit anti-GST antibodies were gifts from K. Kaibuchi (Nagoya University, Aichi, Japan). The rabbit anti-MBP antibodies were purchased from New England Biolabs (Beverly, MA). The mouse anti-HA (HA.11) and

anti-Myc (9E10) monoclonal antibodies were purchased from BAbCO (Richmond, CA) and Sigma-Aldrich (St. Louis, MO), respectively. The horseradish peroxidase-conjugated secondary antibodies (sheep anti-mouse IgG and donkey anti-rabbit IgG) were purchased from GE Healthcare.

Microscopic observations

Cells were observed using a Nikon ECLIPSE E800 microscope (Nikon Instec, Tokyo, Japan) equipped with an HB-10103AF superhigh-pressure mercury lamp and a 1.4 numerical aperture 100x Plan Apo oil immersion objective lens (Nikon Instec) with appropriate fluorescence filter sets (Nikon Instec) or differential interference contrast (DIC) optics. Images were acquired using a cooled digital charge-coupled device camera (C4742-95-12NR; Hamamatsu Photonics, Hamamatsu, Japan) and AQUACOSMOS software (Hamamatsu Photonics). To visualize GFP- or mRFP1-tagged proteins, cells were grown to early to mid-logarithmic phase, harvested, and resuspended in SD medium. Cells were mounted on microslide glass and observed using a GFP bandpass or G-2A (for mRFP1) filter set.

RESULTS

Rcy1p directly interacts with the C-terminal cytoplasmic region of Drs2p

Previously, Furuta *et al*. demonstrated that Rcy1p coimmunoprecipitated with the Cdc50p-Drs2p complex (*5*), but it was not determined which cytoplasmic region of Cdc50p or Drs2p interacts with Rcy1p. Cdc50p and Drs2p have 2 and 10 membrane-spanning regions, respectively (*6,9*). Since the amino-terminal (N-terminal) and C-terminal regions of both proteins are predicted to face the cytoplasm, two-hybrid interaction with Rcy1p was examined for these regions. As shown in **Fig. 3A**, Rcy1p interacted with the C-terminal region of Drs2p, Drs2p(1216-1355), but not with the N-terminal region. To test whether Rcy1p directly binds to Drs2p(1216-1355), pull-down assay was performed. Rcy1p(178-836), which interacted with Drs2p(1216-1355) in two-hybrid (**Fig. 4A**), was fused to GST and the fusion protein was expressed in *E. coli* and purified. Bacterial lysates containing an MBP-Drs2p(1216-1355) fusion protein were incubated with GST-Rcy1p(178-836) immobilized on the glutathione-Sepharose beads, and then the protein complexes bound to glutathione-Sepharose were subjected to western blotting using anti-GST and -MBP antibodies. MBP-Drs2p(1216-1355) bound to GST-Rcy1p(178-836), but not to control GST, whereas control MBP-Rga1p, a fusion with an unrelated protein Rga1p, did not bind to GST-Rcy1p(178-836) (**Fig. 3B**). These results indicate that Rcy1p(178-836) directly interacts with Drs2p(1216-1355). I hereafter refer to Drs2p(1216-1355) as Drs2p-C.

The Drs2p-interacting region of Rcy1p is essential for Rcy1p function

I next examined the Drs2p-binding region in Rcy1p using deletion constructs of Rcy1p (**Fig. 4A**). Drs2p(1216-1355) interacted with Rcy1p(574-836) and Rcy1p(178-778), suggesting that the Drs2p-interacting region resides in amino acid residues 574 to 778 of Rcy1p. Rcy1p(252-836) and Rcy1p(313-836) did not interact with Drs2p, although these proteins were expressed (data not shown). They might not be properly folded, but it is also possible that the upstream region of the Drs2p-interacting region plays a negative regulatory role for the interaction with Drs2p, and this inhibition is released in the full-length Rcy1p.

To examine functional importance of the Drs2p-interacting region, a mutant *RCY1* lacking the amino acid residues 574 to 778 was constructed and expressed in the *rcy1*Δ mutant. The *rcy1*Δ mutant exhibits a defect in the endocytic recycling pathway. A v-SNARE Snc1p is recycled from the plasma membrane via early endosomes to the TGN through this pathway (*30*). In growing wild-type cells, Snc1p is localized to the plasma membrane in polarized sites such as a bud or a cytokinesis site, but it is mislocalized to intracellular endosomal membranes in the *rcy1*Δ mutants (*5,16*). I examined localization of mRFP1-Snc1p in *rcy1*Δ cells carrying the wild-type *RCY1* or *rcy1(*Δ*574-778)* mutant gene on a multicopy plasmid. As shown in **Fig. 4B**, the wild-type *RCY1* cells exhibited polarized localization of mRFP1-Snc1p, but the *rcy1(*Δ*574-778)* mutant cells intracellularly accumulated mRFP1-Snc1p (94% of the cells, n=68) as the *rcy1*Δ mutant did (vector, 95% of the cells, n=43). Expression of Rcy1p(Δ574-778) was confirmed by western blotting (**Fig. 4C**). These results suggest that the interaction with Drs2p is important for Rcy1p function in the endocytic recycling pathway.

Isolation of drs2 mutants that abolished the interaction with Rcy1p

To further investigate the physiological significance of the interaction between Drs2p and Rcy1p, I isolated *drs2* mutants that reduced the interaction with Rcy1p by reverse two-hybrid screening. Two mutants, *drs2-C-M13* and *-M20*, were isolated along with *drs2-C-M3* and *drs2-C-M10* that exhibited a weak interaction with Rcy1p (**Fig. 5A**). Protein levels of these mutants were comparable to that of wild-type Drs2p-C (**Fig. 5A**). I examined the interaction between these Drs2p mutants and Rcy1p by pull-down assay as described in **Fig. 3B**. Consistent with the results by two-hybrid, neither MBP-Drs2p-C-M13 nor MBP-Drs2p-C-M20 bound to GST-Rcy1p(178-836), although MBP-Drs2p-C-M3 and MBP-Drs2p-C-M10 bound to GST-Rcy1p(178-836) to a level comparable to that of the wild type (**Fig. 5B**).

DNA sequencing revealed that each mutant contained multiple amino acid substitutions (**Fig. 5C**). I determined the amino acid substitution that is responsible for the defective interaction with Rcy1p by the two-hybrid method (**Fig. 5D**). Drs2p-C-M3 contained three amino acid substitutions, Q1267R, S1278T, and G1283V, in which Q1267R was responsible for the weak interaction with Rcy1p. Similarly, in Drs2p-C-M10, Q1265H caused reduced interaction with Rcy1p, although Q1265H in combination with S1247N restored the interaction. Drs2p-C-M13 contained 6 amino acid substitutions, in which I1260T abolished the interaction with Rcy1p. Drs2p-C-M20 contained three amino acid substitutions, in which R1264G abolished the interaction. Thus, all amino acid substitutions responsible for the reduced interaction with Rcy1p cluster within an 8-amino acid stretch (amino acids 1260-1267).

The region of Drs2p required for the interaction with Rcy1p is shown in **Fig. 6A**. I noticed that this region is rich in charged (basic) residues that are conserved in fungi (diamonds). Because arginine 1264, which was identified as R1264G, is contained in these basic residues, other basic amino acids might also be involved in the interaction with Rcy1p. I made mutations of these basic residues to alanine to examine their interaction with Rcy1p. R1261A and R1268A resulted in the loss of interaction with Rcy1p, whereas K1262A, K1270A, and K1271A normally interacted (**Fig. 6B**). Protein levels of these mutants were comparable to that of wild-type Drs2p-C (**Fig. 6B**).

I next examined the point mutants of Drs2p, which showed reduced interaction with Rcy1p, in coimmunoprecipitation experiments with Rcy1p as described previously (*5*). I constructed a strain expressing a C-terminally Myc-tagged full-length version of the mutant Drs2p from a low-copy plasmid and an N-terminally HA-tagged full-length version of Rcy1p from a high-copy plasmid. Drs2p-Myc was immunoprecipitated with an anti-Myc antibody from membrane protein extracts prepared by solubilization in 1% CHAPS. The resulting immunoprecipitates were examined by western blotting with anti-Myc and -HA antibodies. HA-Rcy1p was coimmunoprecipitated with wild-type Drs2p-Myc, but not with the I1260T, R1261A, R1264G or R1268A mutant, although a faint interaction was observed with these mutants (**Fig. 6C**). These results suggest that these Drs2p point mutants are also impaired in the *in vivo* interaction with Rcy1p.

Combinations of the drs2 point mutants result in functional defects

I next examined the functionality of *drs2* point mutants containing single amino acid

substitutions that affected interaction with Rcy1p. The *drs2*Δ mutant exhibits cold-sensitive growth at 18°C (*31*) as well as a defect in the endocytic recycling pathway. Snc1p is mislocalized to intracellular endosomal membranes in the *drs2*Δ mutant (*5,7*). I first examined the cold-sensitive growth phenotype of the *drs2* point mutants (**Fig. 7A)**. *drs2-Q1265H* and *drs2-Q1267R*, which only weakly impaired the two-hybrid interaction with Rcy1p, and *drs2-K1262A, drs2-K1270A,* and *drs2-K1271A,* which interacted with Rcy1p in two-hybrid, exhibited normal growth at 18°C. The other four mutants, *drs2-I1260T, drs2-R1264G*, *drs2-R1261A,* and *drs2-R1268A* did not interact with Rcy1p in either two-hybrid or coimmunoprecipitation experiments. However, *drs2-I1260T* and *drs2-R1261A* exhibited almost normal growth, and *drs2-R1264G* and *drs2-R1268A* exhibited partial defects in growth at 18°C.

I reasoned that these *drs2* point mutants might not be completely defective in the interaction with Rcy1p, because faint interactions were observed in the coimmunoprecipitation experiments in **Fig. 6C**. I then constructed combinations (double mutations) of these four mutations to examine their phenotypes. Interestingly, four of these double mutants exhibited mild or severe defects in growth at 18°C and endocytic recycling of GFP-Snc1p: *drs2-I1260T/R1268A* and *drs2-R1261A/R1264G* mutants were partially defective, whereas *drs2-I1260T/R1264G* and *drs2-R1264G/R1268A* were completely defective in these phenotypes (**Fig. 7B and D**). Protein levels of these mutants were confirmed to be comparable to that of wild-type Drs2p (**Fig. 7C**). All these loss-of-function mutants contained the R1264G or R1268A substitution, which exhibited partial defects in growth at 18°C. The mutant with both substitutions, *drs2-R1264G/R1268A*, exhibited slow

growth even at 30°C like the *drs2*Δ mutant. I next examined whether one of the completely defective mutants, Drs2p-I1260T/R1264G, is impaired in the interaction with Rcy1p by co-immunoprecipitation experiments. Unexpectedly, Drs2p-I1260T/R1264G weakly interacted with HA-Rcy1p to an extent similar to that with Drs2p-I1260T and Drs2p-R1264G single mutants (**Fig. 7E**). These results suggest that there is a second weak interaction site in the Drs2p C-terminal region, or that the interaction surface of Drs2p is not completely impaired by mutations in the small amino acids 1260 to 1268 region. Nonetheless, the complete loss of function of the *drs2-I1260T/R1264G* mutant suggests that this region performs an important function by interacting with Rcy1p.

These results indicate that the amino acids 1260 to 1268 of Drs2p are functionally important. I propose that the interaction of Drs2p with Rcy1p is important for the Drs2p function in the endocytic recycling pathway.

Endosomal localization of GFP-Rcy1p may be dependent on the interaction with Drs2p

Furuta *et al*. previously showed that GFP-Rcy1p was colocalized with mRFP1-Drs2p (*5*). Thus, the results described above raise a possibility that Rcy1p is recruited to endosomal membranes through the interaction with the C-terminal region of Drs2p. mRFP1-Snc1p and GFP-Rcy1p were expressed in wild-type, *drs2-I1260T/R1264G*, and *drs2*Δ mutant cells, and their localizations were examined. In wild-type cells, GFP-Rcy1p was observed in punctate structures scattered throughout the cell, whereas mRFP1-Snc1p was primarily localized to the plasma membrane, with a small fraction observed in intracellular punctate structures, which were shown to be endosomal/TGN membranes (*30*) (**Fig. 8A**). Some

GFP-Rcy1p dots were colocalized with these mRFP1-Snc1 dots. In *drs2-I1260T/R1264G* and *drs2*Δ mutant cells, mRFP1-Snc1p was accumulated in the early endosome-derived structures, while GFP-Rcy1p was independent of these mRFP1-Snc1p structures (**Fig. 8A**). I also examined localization of Drs2p-I1260T/R1264G-GFP. When expressed in wild-type cells, it exhibited normal punctate localization (**Fig. 9**), indicating that it associated with Cdc50p and was normally localized to endosomal/TGN membranes (*4*). In the *drs2*Δ mutant, Drs2p-I1260T/R1264G-GFP was localized to the mRFP1-Snc1p-containing structures (**Fig. 8B**). These results are consistent with a notion that GFP-Rcy1p is localized to early endosomal membranes via the interaction with Drs2p. These results also suggest that GFP-Rcy1p is localized to some internal membranes in addition to early endosomes. I examined the colocalization of GFP-Rcy1p with Sec7p-mRFP1, a TGN marker, in wild-type and *drs2*Δ cells (**Fig. 8C**). In wild-type cells, 23% of GFP-Rcy1p-positive structures were Sec7p-mRFP1 positive (n=80). Conversely, 18% of Sec7p-mRFP1 structures were GFP-Rcy1p positive (n=80). In the *drs2*Δ cells, 37% of GFP-Rcy1p structures were Sec7p-mRFP1 positive (n=80), whereas 20% of Sec7p-mRFP1 structures were GFP-Rcy1p positive (n=80). These results suggest that GFP-Rcy1p is localized to TGN membranes in addition to early endosomes in a Drs2p-independent manner.

DISCUSSION

Here I show that Rcy1p directly interacts with the C-terminal cytoplasmic region of Drs2p at its C-terminal amino acids 574 to 778 region (**Fig. 3 and Fig. 4**). Random and site-directed mutagenesis of the C-terminal region of Drs2p revealed that at least a nine amino acid region, isoleucine 1260 to arginine 1268, is required for the interaction with Rcy1p (**Fig. 5 and Fig. 6**). Single substitution mutants of this region did not exhibit major defects in the Drs2p function, but combinatory mutations containing R1264G or R1268A resulted in clear defects in both growth at 18°C and endocytic recycling of GFP-Snc1p like the *drs2*Δ mutant (**Fig. 7**). These results suggest that the interaction with Rcy1p is important for Drs2p to promote the early endosome-to-TGN transport of Snc1p.

It was previously shown that the C-terminal region of Drs2p also bound to the Sec7 domain of Gea2p, a guanine nucleotide exchange factor for the Arf1p small GTPase (*32*). Interestingly, the Rcy1p-interacting region of Drs2p (amino acids 1260-1268) overlaps with the Gea2p-interacting region (amino acids 1250-1270). My two-hybrid results indicated that the I1260T and R1264G substitutions also impaired interactions with Gea2p, suggesting that Rcy1p and Gea2p may not simultaneously interact with the same molecule of Drs2p (data not shown). Gea2p is implicated in the secretory pathway (*33*) and may cooperate with Arl1p (Arf-like protein) to regulate Drs2p flippase activity at the TGN (*34*). Therefore, Drs2p localized at early endosomes may preferentially interact with Rcy1p, whereas Drs2p at the Golgi may do so with Gea2p. In addition to Rcy1p, the C-terminal region of Drs2p interacted with PtdIns(4)P and this interaction stimulated the flippase activity of Drs2p (*35*). Interestingly, the potential PtdIns(4)P-binding region of Drs2p

(amino acids 1268-1273) is just downstream of the Rcy1p- and Gea2p-interacting regions, suggesting that the PtdIns(4)P binding could affect interaction with Rcy1p and *vice versa*.

Furuta *et al*. previously showed that Drs2p was colocalized with Rcy1p (*5*). In this colocalization, 49% of Drs2p-mRFP1 dots contained the GFP-Rcy1p signal, suggesting that the interaction of Drs2p with Rcy1p is regulated. The Rab family small GTPases Ypt31/32p could regulate this interaction, because Rcy1p was shown to be a potential effector of Ypt31/32p (*17*). However, I could not detect any difference in the amount of Rcy1p coimmunoprecipitated with Drs2p between wild-type and temperature-sensitive *ypt31 ypt32* strains (preliminary data). In the *drs2-I1260T/R1264G* and *drs2*Δ mutants, GFP-Rcy1p was not localized to accumulated endosomal membranes, implying that the interaction with Drs2p is required for localization of Rcy1p to early endosomes (**Fig. 8**). On the other hand, GFP-Rcy1p was still localized to dotty structures in the *drs2*Δ mutant, suggesting that there is another factor that recruits GFP-Rcy1p to the membranes (**Fig. 8**). Consistently, 26% of the GFP-Rcy1p positive structures were not colocalized with Drs2p-mRFP1 (*5*). Because some of the GFP-Rcy1p dots were colocalized with Sec7p-mRFP1, these structures seem to be TGN membranes. The functions of Rcy1p in TGN membranes need to be investigated.

Cdc50p-Drs2p has been implicated in the formation of clathrin-coated vesicles, and AP-1 is a candidate adaptor for this process (*13*,*14*). One possible function of Rcy1p is to spatiotemporally coordinate phospholipid flipping, cargo recruitment, and adaptor recruitment at the site where Drs2p is flipping phospholipids (**Fig. 10**). Defects in this Rcy1p function would result in random distribution of cargos on endosomal membranes.

Although AP-1 may function downstream of Drs2p, both *drs2*Δ and *rcy1*Δ mutants exhibit substantial defects in the endocytic recycling pathway, but the mutants in AP-1 do not, suggesting that there is another adaptor that is involved in the vesicle formation by Drs2p. Alternatively, Rcy1p by itself may perform an adaptor function, because Rcy1p physically interacted with Snc1p (*17*).

It was suggested that Rcy1p forms a non-SCF complex with Skp1p, because Rcy1p interacted with Skp1p at its F-box domain, but not with Cdc53p/cullin (*16*). On the other hand, Rcy1p was shown to form an SCF complex *in vitro*, by which Rcy1p was auto-ubiquitinated in the presence of the E2 enzyme Cdc34p (*20*). In addition, Snc1p was ubiquitinated *in vivo* in an Rcy1p-dependent manner, and this ubiquitination was implicated in recycling of Snc1p (*36*). If Rcy1p is involved in the ubiquitination reaction, its functional relationship to Drs2p would be a next challenge.

REFERENCES

1. Lenoir, G., Williamson, P., and Holthuis, J. C. (2007) On the origin of lipid asymmetry: the flip side of ion transport. *Curr. Opin. Chem. Biol.* **11**, 654-661
2. Tanaka, K., Fujimura-Kamada, K., and Yamamoto, T. (2011) Functions of phospholipid flippases. *J. Biochem.* **149**, 131-143
3. Sebastian, T. T., Baldridge, R. D., Xu, P., and Graham, T. R. (2012) Phospholipid flippases: Building asymmetric membranes and transport vesicles. *Biochim. Biophys. Acta* **1821**, 1068-1077
4. Saito, K., Fujimura-Kamada, K., Furuta, N., Kato, U., Umeda, M., and Tanaka, K. (2004) Cdc50p, a protein required for polarized growth, associates with the Drs2p P-type ATPase implicated in phospholipid translocation in *Saccharomyces cerevisiae*. *Mol. Biol. Cell* **15**, 3418-3432
5. Furuta, N., Fujimura-Kamada, K., Saito, K., Yamamoto, T., and Tanaka, K. (2007) Endocytic recycling in yeast is regulated by putative phospholipid translocases and the Ypt31p/32p-Rcy1p pathway. *Mol. Biol. Cell* **18**, 295-312
6. Chen, C. Y., Ingram, M. F., Rosal, P. H., and Graham, T. R. (1999) Role for Drs2p, a P-type ATPase and potential aminophospholipid translocase, in yeast late Golgi function. *J. Cell Biol.* **147**, 1223-1236
7. Hua, Z., Fatheddin, P., and Graham, T. R. (2002) An essential subfamily of Drs2p-related P-type ATPases is required for protein trafficking between Golgi complex and endosomal/vacuolar system. *Mol. Biol. Cell* **13**, 3162-3177
8. Pomorski, T., Lombardi, R., Riezman, H., Devaux, P. F., van Meer, G., and Holthuis, J. C. (2003) Drs2p-related P-type ATPases Dnf1p and Dnf2p are required for phospholipid translocation across the yeast plasma membrane and serve a role in endocytosis. *Mol. Biol. Cell* **14**, 1240-1254
9. Misu, K., Fujimura-Kamada, K., Ueda, T., Nakano, A., Katoh, H., and Tanaka, K. (2003) Cdc50p, a conserved endosomal membrane protein, controls polarized growth in *Saccharomyces cerevisiae*. *Mol. Biol. Cell* **14**, 730-747
10. Kelly, B. T., and Owen, D. J. (2011) Endocytic sorting of transmembrane protein cargo. *Curr. Opin. Cell Biol.* **23**, 404-412
11. Valdivia, R. H., Baggott, D., Chuang, J. S., and Schekman, R. W. (2002) The yeast clathrin adaptor protein complex 1 is required for the efficient retention of a subset

of late Golgi membrane proteins. *Dev. Cell* **2**, 283-294

12. Foote, C., and Nothwehr, S. F. (2006) The clathrin adaptor complex 1 directly binds to a sorting signal in Ste13p to reduce the rate of its trafficking to the late endosome of yeast. *J. Cell Biol.* **173**, 615-626
13. Sakane, H., Yamamoto, T., and Tanaka, K. (2006) The functional relationship between the Cdc50p-Drs2p putative aminophospholipid translocase and the Arf GAP Gcs1p in vesicle formation in the retrieval pathway from yeast early endosomes to the TGN. *Cell Struct. Funct.* **31**, 87-108
14. Liu, K., Surendhran, K., Nothwehr, S. F., and Graham, T. R. (2008) P4-ATPase requirement for AP-1/clathrin function in protein transport from the *trans*-Golgi network and early endosomes. *Mol. Biol. Cell* **19**, 3526-3535
15. Wiederkehr, A., Avaro, S., Prescianotto-Baschong, C., Haguenauer-Tsapis, R., and Riezman, H. (2000) The F-box protein Rcy1p is involved in endocytic membrane traffic and recycling out of an early endosome in *Saccharomyces cerevisiae*. *J. Cell Biol.* **149**, 397-410
16. Galan, J. M., Wiederkehr, A., Seol, J. H., Haguenauer-Tsapis, R., Deshaies, R. J., Riezman, H., and Peter, M. (2001) Skp1p and the F-box protein Rcy1p form a non-SCF complex involved in recycling of the SNARE Snc1p in yeast. *Mol. Cell. Biol.* **21**, 3105-3117
17. Chen, S. H., Chen, S., Tokarev, A. A., Liu, F., Jedd, G., and Segev, N. (2005) Ypt31/32 GTPases and their novel F-box effector protein Rcy1 regulate protein recycling. *Mol. Biol. Cell* **16**, 178-192
18. Jackson, P. K., and Eldridge, A. G. (2002) The SCF ubiquitin ligase: an extended look. *Mol. Cell* **9**, 923-925
19. Cardozo, T., and Pagano, M. (2004) The SCF ubiquitin ligase: insights into a molecular machine. *Nat. Rev. Mol. Cell Biol.* **5**, 739-751
20. Kus, B. M., Caldon, C. E., Andorn-Broza, R., and Edwards, A. M. (2004) Functional interaction of 13 yeast SCF complexes with a set of yeast E2 enzymes *in vitro*. *Proteins* **54**, 455-467
21. Rose, M. D., Winston, F., and Hieter, P. (1990) *Methods in Yeast Genetics: A Laboratory Course Manual*, Cold Spring Harbor Laboratory Press, Cold Spring Harbor, NY
22. Guthrie, C. and Fink, G. R. (1991) *Guide to Yeast Genetics and Molecular Biology*,

Academic Press, San Diego, CA

23. Elble, R. (1992) A simple and efficient procedure for transformation of yeasts. *Biotechniques* **13**, 18-20
24. Gietz, R. D., and Woods, R. A. (2002) Transformation of yeast by lithium acetate/single-stranded carrier DNA/polyethylene glycol method. *Methods Enzymol.* **350**, 87-96
25. Goldstein, A. L., and McCusker, J. H. (1999) Three new dominant drug resistance cassettes for gene disruption in *Saccharomyces cerevisiae*. *Yeast* **15**, 1541-1553
26. Hollenberg, S. M., Sternglanz, R., Cheng, P. F., and Weintraub, H. (1995) Identification of a new family of tissue-specific basic helix-loop-helix proteins with a two-hybrid system. *Mol. Cell. Biol.* **15**, 3813-3822
27. Durfee, T., Becherer, K., Chen, P. L., Yeh, S. H., Yang, Y., Kilburn, A. E., Lee, W. H., and Elledge, S. J. (1993) The retinoblastoma protein associates with the protein phosphatase type 1 catalytic subunit. *Genes Dev.* **7**, 555-569
28. Toi, H., Fujimura-Kamada, K., Irie, K., Takai, Y., Todo, S., and Tanaka, K. (2003) She4p/Dim1p interacts with the motor domain of unconventional myosins in the budding yeast, *Saccharomyces cerevisiae*. *Mol. Biol. Cell* **14**, 2237-2249
29. Ho, S. N., Hunt, H. D., Horton, R. M., Pullen, J. K., and Pease, L. R. (1989) Site-directed mutagenesis by overlap extension using the polymerase chain reaction. *Gene* **77**, 51-59
30. Lewis, M. J., Nichols, B. J., Prescianotto-Baschong, C., Riezman, H., and Pelham, H. R. (2000) Specific retrieval of the exocytic SNARE Snc1p from early yeast endosomes. *Mol. Biol. Cell* **11**, 23-38
31. Ripmaster, T. L., Vaughn, G. P., and Woolford, J. L., Jr. (1993) *DRS1* to *DRS7*, novel genes required for ribosome assembly and function in *Saccharomyces cerevisiae*. *Mol. Cell. Biol.* **13**, 7901-7912
32. Chantalat, S., Park, S. K., Hua, Z., Liu, K., Gobin, R., Peyroche, A., Rambourg, A., Graham, T. R., and Jackson, C. L. (2004) The Arf activator Gea2p and the P-type ATPase Drs2p interact at the Golgi in *Saccharomyces cerevisiae*. *J. Cell Sci.* **117**, 711-722
33. Park, S. K., Hartnell, L. M., and Jackson, C. L. (2005) Mutations in a highly conserved region of the Arf1p activator *GEA2* block anterograde Golgi transport but not COPI recruitment to membranes. *Mol. Biol. Cell* **16**, 3786-3799

34. Tsai, P. C., Hsu, J. W., Liu, Y. W., Chen, K. Y., and Lee, F. J. (2013) Arl1p regulates spatial membrane organization at the *trans*-Golgi network through interaction with Arf-GEF Gea2p and flippase Drs2p. *Proc. Natl. Acad. Sci. USA* **110**, E668-E677

35. Natarajan, P., Liu, K., Patil, D. V., Sciorra, V. A., Jackson, C. L., and Graham, T. R. (2009) Regulation of a Golgi flippase by phosphoinositides and an ArfGEF. *Nat. Cell Biol.* **11**, 1421-1426

36. Chen, S. H., Shah, A. H., and Segev, N. (2011) Ypt31/32 GTPases and their F-Box effector Rcy1 regulate ubiquitination of recycling proteins. *Cell. Logist.* **1**, 21-31

37. Gietz, R. D., and Sugino, A. (1988) New yeast-*Escherichia coli* shuttle vectors constructed with *in vitro* mutagenized yeast genes lacking six-base pair restriction sites. *Gene* **74**, 527-534

38. James, P., Halladay, J., and Craig, E. A. (1996) Genomic libraries and a host strain designed for highly efficient two-hybrid selection in yeast. *Genetics* **144**, 1425-1436

39. Imamura, H., Tanaka, K., Hihara, T., Umikawa, M., Kamei, T., Takahashi, K., Sasaki, T., and Takai, Y. (1997) Bni1p and Bnr1p: downstream targets of the Rho family small G-proteins which interact with profilin and regulate actin cytoskeleton in *Saccharomyces cerevisiae*. *EMBO J.* **16**, 2745-2755

ACKNOWLEDGEMENTS

I am deeply grateful to Dr. Kazuma Tanaka, Dr. Konomi Fujimura-Kamada and Dr. Takaharu Yamamoto whose tutelages and suggestions were of inestimable value for my study. I also owe a very important debt to Dr. Hideaki Higashi and Dr. Naomi Ohnishi who provided sincere encouragement. The member of the Tanaka laboratory gave me insightful comments. Eriko Itoh's technical assistance was an enormous help to me. My deepest appreciation goes to my family for their moral support and warm encouragements.

Table I. *S. cerevisiae* strains used in this study

Strain	Genotype	Reference and source
L40	*MAT***a** *his3-200 trp1-901 leu2-3,112 ade2 LYS2::(lexAop)4-HIS3 URA3::(lexAop)8-lacZ*	*(27)*
YKT38	*MAT***a** *lys2-801 ura3Δ-52 his3Δ-200 trp1Δ-63 leu2Δ-1*	*(9)*
YKT746	*MAT***a** *lys2-801 ura3Δ-52 his3Δ-200 trp1Δ-63 leu2Δ-1 drs2Δ::kanMX4*	This study
YKT905	*MAT***a** *lys2-801 ura3Δ-52 his3Δ-200 trp1Δ-63 leu2Δ-1 SEC7-mRFP1::TRP1*	*(13)*
YKT951	*MAT***a** *lys2-801 ura3Δ-52 his3Δ-200 trp1Δ-63 leu2Δ-1 rcy1Δ::kanMX4*	*(5)*
YKT1096	*MAT***a** *lys2-801 ura3Δ-52 his3Δ-200 trp1Δ-63 leu2Δ-1 rcy1Δ::hphMX4*	This study
YKT1778	*MAT*α *lys2-801 ura3Δ-52 his3Δ-200 trp1Δ-63 LEU2::mRFP1-SNC1*	This study
YKT1780	*MAT***a** *lys2-801 ura3Δ-52 his3Δ-200 trp1Δ-63 rcy1Δ::hphMX4 LEU2::mRFP1-SNC1*	This study
YHH22	*MAT***a** *his3-200 trp1-901 leu2-3,112 ade2 LYS2::(lexAop)4-HIS3 URA3::(lexAop)8-lacZ* **[**pBTM116-HA-RCY1ΔCAAX**]**	This study
YHH636	*MAT*α *lys2-801 ura3Δ-52 his3Δ-200 trp1Δ-63 leu2Δ-1 drs2Δ::kanMX4 SEC7-mRFP1::TRP1*	This study

Table II. Plasmids used in this study

Plasmid	Characteristics	Reference and Source
pRS305-mRFP1-SNC1	*P_{TPI}-mRFP1-SNC1 LEU2*	This study
YEplac112	*TRP1 2μm*	*(37)*
pKT2054 [YEplac112-GFP-RCY1]	*GFP-RCY1 TRP1 2μm*	This study
YEplac195	*URA3 2μm*	*(37)*
pKT1443 [pRS416-GFP-SNC1]	*P_{TPI}-GFP-SNC1 URA3 CEN*	*(30)*
pKT1560 [YEplac181-GFP-RCY1]	*GFP-RCY1 LEU2 2μm*	*(5)*
pKT1563 [pRS416-mRFP1-SNC1]	*P_{TPI}-mRFP1-SNC1 URA3 CEN*	*(5)*
pKT1626 [YEplac195-3HA-BS-RCY1]	*3HA-RCY1 URA3 2μm*	*(5)*
pKT2053 [YEplac195-3HA-BS-RCY1(Δ574-778)]	*3HA-RCY1(Δ574-778) URA3 2μm*	This study
pGAD-C1	*AD_{GAL4}[a] LEU2 2μm*	*(38)*
pKT1612 [pGAD-C1-CDC50(1-50)]	*AD_{GAL4}-CDC50(1-50) LEU2 2μm*	This study
pKT1728 [pGAD-C1-CDC50(353-391)]	*AD_{GAL4}-CDC50(353-391) LEU2 2μm*	This study
pKT1610 [pGAD-C1-DRS2(1-225)]	*AD_{GAL4}-DRS2(1-225) LEU2 2μm*	This study
pKT1611 [pGAD-C1-DRS2(1216-1355)]	*AD_{GAL4}-DRS2(1216-1355) LEU2 2μm*	This study
pKT1865 [pGAD-C1-2HA-DRS2(1216-1355)]	*AD_{GAL4}-2HA-DRS2(1216-1355) LEU2 2μm*	This study
pKT1866 [pGAD-C1-2HA-DRS2(1216-1355)-M3]	*AD_{GAL4}-2HA-DRS2(1216-1355)-M3 LEU2 2μm*	This study
pKT1867 [pGAD-C1-2HA-DRS2(1216-1355)-M10]	*AD_{GAL4}-2HA-DRS2(1216-1355)-M10 LEU2 2μm*	This study
pKT1868 [pGAD-C1-2HA-DRS2(1216-1355)-M13]	*AD_{GAL4}-2HA-DRS2(1216-1355)-M13 LEU2 2μm*	This study
pKT1869 [pGAD-C1-2HA-DRS2(1216-1355)-M20]	*AD_{GAL4}-2HA-DRS2(1216-1355)-M20 LEU2 2μm*	This study
pKT1909 [pGAD-C1-2HA-DRS2(1216-1355)-R1261A]	*AD_{GAL4}-2HA-DRS2(1216-1355)-R1261A LEU2 2μm*	This study
pKT1910 [pGAD-C1-2HA-DRS2(1216-1355)-K1262A]	*AD_{GAL4}-2HA-DRS2(1216-1355)-K1262A LEU2 2μm*	This study
pKT1911 [pGAD-C1-2HA-DRS2(1216-1355)-R1268A]	*AD_{GAL4}-2HA-DRS2(1216-1355)-R1268A LEU2 2μm*	This study
pKT1912 [pGAD-C1-2HA-DRS2(1216-1355)-K1270A]	*AD_{GAL4}-2HA-DRS2(1216-1355)-K1270A LEU2 2μm*	This study
pKT1913 [pGAD-C1-2HA-DRS2(1216-1355)-K1271A]	*AD_{GAL4}-2HA-DRS2(1216-1355)-K1271A LEU2 2μm*	This study
pGAD-C1-2HA-DRS2(1216-1355)-I1260T	*AD_{GAL4}-2HA-DRS2(1216-1355)-I1260T LEU2 2μm*	This study
pGAD-C1-2HA-DRS2(1216-1355)-R1264G	*AD_{GAL4}-2HA-DRS2(1216-1355)-R1264G LEU2 2μm*	This study
pGAD-C1-2HA-DRS2(1216-1355)-Q1267R	*AD_{GAL4}-2HA-DRS2(1216-1355)-Q1267R LEU2 2μm*	This study
pGAD-C1-2HA-DRS2(1216-1355)-Q1267R/G1283V	*AD_{GAL4}-2HA-DRS2(1216-1355)-Q1267R/G1283V LEU2 2μm*	This study
pGAD-C1-2HA-DRS2(1216-1355)-S1278T/G1283V	*AD_{GAL4}-2HA-DRS2(1216-1355)-S1278T/G1283V LEU2 2μm*	This study
pGAD-C1-2HA-DRS2(1216-1355)-Q1267R/S1278P	*AD_{GAL4}-2HA-DRS2(1216-1355)-Q1267R/S1278P LEU2 2μm*	This study
pGAD-C1-2HA-DRS2(1216-1355)-G1283V	*AD_{GAL4}-2HA-DRS2(1216-1355)-G1283V LEU2 2μm*	This study

pGAD-C1-2HA-DRS2(1216-1355)-S1247N	*AD_{GAL4}-2HA-DRS2(1216-1355)-S1247N LEU2 2μm*	This study
pGAD-C1-2HA-DRS2(1216-1355)-Q1265H	*AD_{GAL4}-2HA-DRS2(1216-1355)-Q1265H LEU2 2μm*	This study
pGAD-C1-2HA-DRS2(1216-1355)-F1275C	*AD_{GAL4}-2HA-DRS2(1216-1355)-F1275C LEU2 2μm*	This study
pGAD-C1-2HA-DRS2(1216-1355)-S1247N/Q1265H	*AD_{GAL4}-2HA-DRS2(1216-1355)-S1247N/Q1265H LEU2 2μm*	This study
pGAD-C1-2HA-DRS2(1216-1355)-Q1265H/F1275C	*AD_{GAL4}-2HA-DRS2(1216-1355)-Q1265H/F1275C LEU2 2μm*	This study
pGAD-C1-2HA-DRS2(1216-1355)-S1278P	*AD_{GAL4}-2HA-DRS2(1216-1355)-S1278P LEU2 2μm*	This study
pGAD-C1-2HA-DRS2(1216-1355)-E1303K	*AD_{GAL4}-2HA-DRS2(1216-1355)-E1303K LEU2 2μm*	This study
pGAD-C1-2HA-DRS2(1216-1355)-F1312Y	*AD_{GAL4}-2HA-DRS2(1216-1355)-F1312Y LEU2 2μm*	This study
pGAD-C1-2HA-DRS2(1216-1355)-T1234M/Y1235H	*AD_{GAL4}-2HA-DRS2(1216-1355)-T1234M/Y1235H LEU2 2μm*	This study
pBTM116-HA	*DBD_{lexA}[b]-HA TRP1 2μm*	*(39)*
pKT1734 [pBTM116-HA-RCY1]	*DBD_{lexA}-HA-RCY1 TRP1 2μm*	This study
pKT1652 [pBTM116-HA-RCY1ΔCAAX]	*DBD_{lexA}-HA-RCY1ΔCAAX TRP1 2μm*	This study
pKT2034 [pBTM116-HA-RCY1(178-836)]	*DBD_{lexA}-HA-RCY1(178-836) TRP1 2μm*	This study
pKT2035 [pBTM116-HA-RCY1(252-836)]	*DBD_{lexA}-HA-RCY1(252-836) TRP1 2μm*	This study
pKT2036 [pBTM116-HA-RCY1(313-836)]	*DBD_{lexA}-HA-RCY1(313-836) TRP1 2μm*	This study
pKT2037 [pBTM116-HA-RCY1(574-836)]	*DBD_{lexA}-HA-RCY1(574-836) TRP1 2μm*	This study
pKT2038 [pBTM116-HA-RCY1(662-836)]	*DBD_{lexA}-HA-RCY1(662-836) TRP1 2μm*	This study
pKT2039 [pBTM116-HA-RCY1(730-836)]	*DBD_{lexA}-HA-RCY1(730-836) TRP1 2μm*	This study
pKT2040 [pBTM116-HA-RCY1(178-478)]	*DBD_{lexA}-HA-RCY1(178-478) TRP1 2μm*	This study
pKT2041 [pBTM116-HA-RCY1(178-669)]	*DBD_{lexA}-HA-RCY1(178-669) TRP1 2μm*	This study
pKT2042 [pBTM116-HA-RCY1(178-724)]	*DBD_{lexA}-HA-RCY1(178-724) TRP1 2μm*	This study
pKT2043 [pBTM116-HA-RCY1(178-778)]	*DBD_{lexA}-HA-RCY1(178-778) TRP1 2μm*	This study
pGEX-4T-1	*GST*	GE healthcare
pKT1876 [pGEX-4T-1-RCY1(178-836)]	*GST-RCY1(178-836)*	This study
pMAL-c2	*MBP*	New England Biolabs
pKT1870 [pMAL-c2-2HA-DRS2(1216-1355)]	*MBP-2HA-DRS2(1216-1355)*	This study
pKT1871 [pMAL-c2-2HA-DRS2(1216-1355)-M3]	*MBP-2HA-DRS2(1216-1355)-M3*	This study
pKT1872 [pMAL-c2-2HA-DRS2(1216-1355)-M10]	*MBP-2HA-DRS2(1216-1355)-M10*	This study
pKT1873 [pMAL-c2-2HA-DRS2(1216-1355)-M13]	*MBP-2HA-DRS2(1216-1355)-M13*	This study
pKT1874 [pMAL-c2-2HA-DRS2(1216-1355)-M20]	*MBP-2HA-DRS2(1216-1355)-M20*	This study
pKT1875 [pMAL-c2-RGA1(768-1007)]	*MBP-RGA1(768-1007)*	This study
YCplac111	*LEU2 CEN*	*(37)*
pKT1860 [YCplac111-DRS2-13Myc-T_{ADH}]	*DRS2-13Myc LEU2 CEN*	This study

pKT1883 [YCplac111-DRS2-I1260T-13Myc-T_{ADH}]	*drs2-I1260T-13Myc LEU2 CEN*	This study
pKT1884 [YCplac111-DRS2-R1264G-13Myc-T_{ADH}]	*drs2-R1264G-13Myc LEU2 CEN*	This study
pKT1906 [YCplac111-DRS2-Q1265H-13Myc-T_{ADH}]	*drs2-Q1265H-13Myc LEU2 CEN*	This study
pKT1907 [YCplac111-DRS2-Q1267R-13Myc-T_{ADH}]	*drs2-Q1267R-13Myc LEU2 CEN*	This study
pKT1908 [YCplac111-DRS2-I1260T/R1264G-13Myc-T_{ADH}]	*drs2-I1260T/R1264G-13Myc LEU2 CEN*	This study
pKT1914 [YCplac111-DRS2-R1261A-13Myc-T_{ADH}]	*drs2-R1261A-13Myc LEU2 CEN*	This study
pKT1915 [YCplac111-DRS2-K1262A-13Myc-T_{ADH}]	*drs2-K1262A-13Myc LEU2 CEN*	This study
pKT1916 [YCplac111-DRS2-R1268A-13Myc-T_{ADH}]	*drs2-R1268A-13Myc LEU2 CEN*	This study
pKT1917 [YCplac111-DRS2-K1270A-13Myc-T_{ADH}]	*drs2-K1270A-13Myc LEU2 CEN*	This study
pKT1918 [YCplac111-DRS2-K1271A-13Myc-T_{ADH}]	*drs2-K1271A-13Myc LEU2 CEN*	This study
pKT2055 [YCplac111-DRS2-I1260T/R1261A-13Myc-T_{ADH}]	*drs2-I1260T/R1261A-13Myc LEU2 CEN*	This study
pKT2056 [YCplac111-DRS2-I1260T/R1268A-13Myc-T_{ADH}]	*drs2-I1260T/R1268A-13Myc LEU2 CEN*	This study
pKT2057 [YCplac111-DRS2-R1261A/R1264G-13Myc-T_{ADH}]	*drs2-R1261A/R1264G-13Myc LEU2 CEN*	This study
pKT2058 [YCplac111-DRS2-R1261A/R1268A-13Myc-T_{ADH}]	*drs2-R1261A/R1268A-13Myc LEU2 CEN*	This study
pKT2059 [YCplac111-DRS2-R1264G/R1268A-13Myc-T_{ADH}]	*drs2-R1264G/R1268A-13Myc LEU2 CEN*	This study
pKT2123 [YCplac111-DRS2-GFP-T_{ADH}]	*Drs2-GFP LEU2 CEN*	This study
pKT2124 [YCplac111-DRS2-I1260T-GFP-T_{ADH}]	*drs2-I1260T-GFP LEU2 CEN*	This study
pKT2125 [YCplac111-DRS2-R1264G-GFP-T_{ADH}]	*drs2-R1264G-GFP LEU2 CEN*	This study
pKT2104 [YCplac111-DRS2-I1260T/R1264G-GFP-T_{ADH}]	*drs2-I1260T/R1264G-GFP LEU2 CEN*	This study

[a] AD_{GAL4} is the transcriptional activating domain of Gal4.

[b] DBD_{LexA} is the DNA-binding domain of LexA.

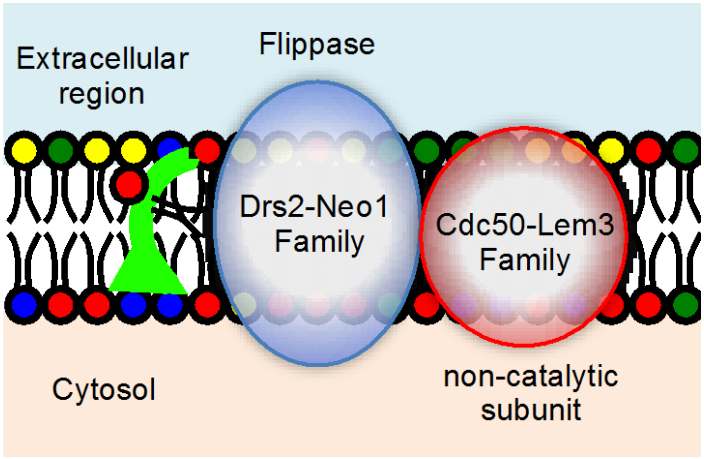

Fig. 1 The type 4 subfamily of P-type ATPases (Flippases).

The type 4 subfamily of P-type ATPases are also called flippases and composed of the Drs2 family catalytic subunits and the Cdc50-Lem3 family non-catalytic subunits. Flippases are implicated in the translocation of phospholipids from the exoplasmic to cytosolic leaflet to generate phospholipid asymmetry in membrane bilayers.

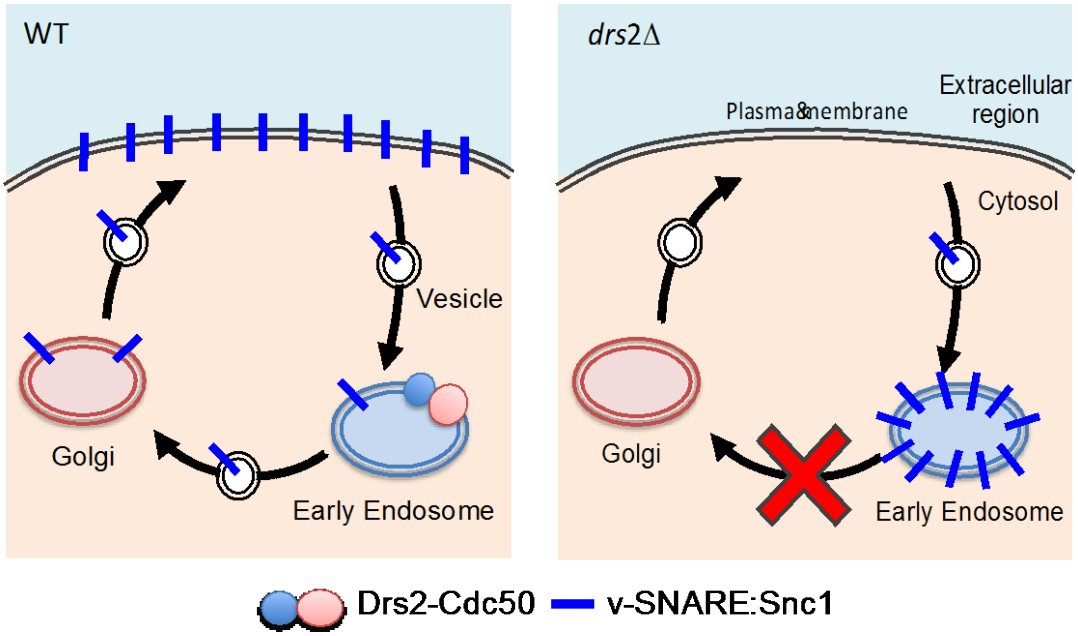

Fig. 2 Localization of GFP-Snc1p in wild-type and *drs*2Δ mutant cells.

Snc1p, a vesicle-soluble N-ethylmaleimide- sensitive factor attachment protein receptor (v-SNARE), is recycled from the plasma membrane *via* early endosomes to the *trans*-Golgi Network (TGN) (Left panel). In the *drs*2Δ mutant, GFP-Snc1 accumulates in the abnormal early endosome-derived structures due to its defects in vesicle formation from early endosomes (Right panel).

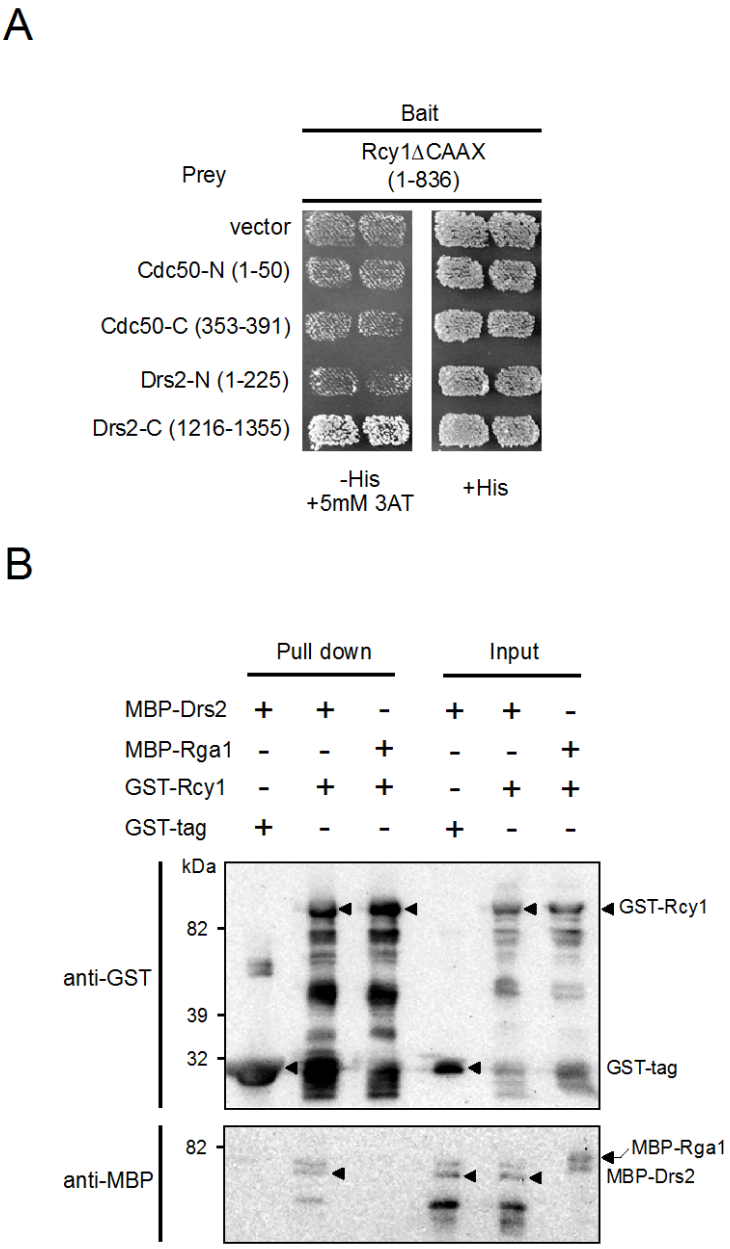

Fig. 3 Rcy1p directly interacts with the C-terminal region of Drs2p.

(A) Rcy1p interacts with Drs2p(1216-1355) in two-hybrid. YHH22, the L40 strain carrying the *RCY1ΔCAAX* bait plasmid (pKT1652), was transformed with prey plasmids carrying the N- or C-terminal region of Drs2p and Cdc50p (pKT1610-1612 and pKT1728). The cells were grown on an SD-Leu-Trp plate without histidine containing 5 mM 3AT for 6 days at 30°C. (B) Drs2p(1216-1355) interacts with Rcy1p(178-836) in pull-down assay. MBP-Drs2p(1216-1355) was precipitated from *E. coli* lysates with GST-Rcy1p(178-836) bound to glutathione beads, followed by western blotting using anti-GST and -MBP antibodies. MBP-Rga1p was used as a

control.

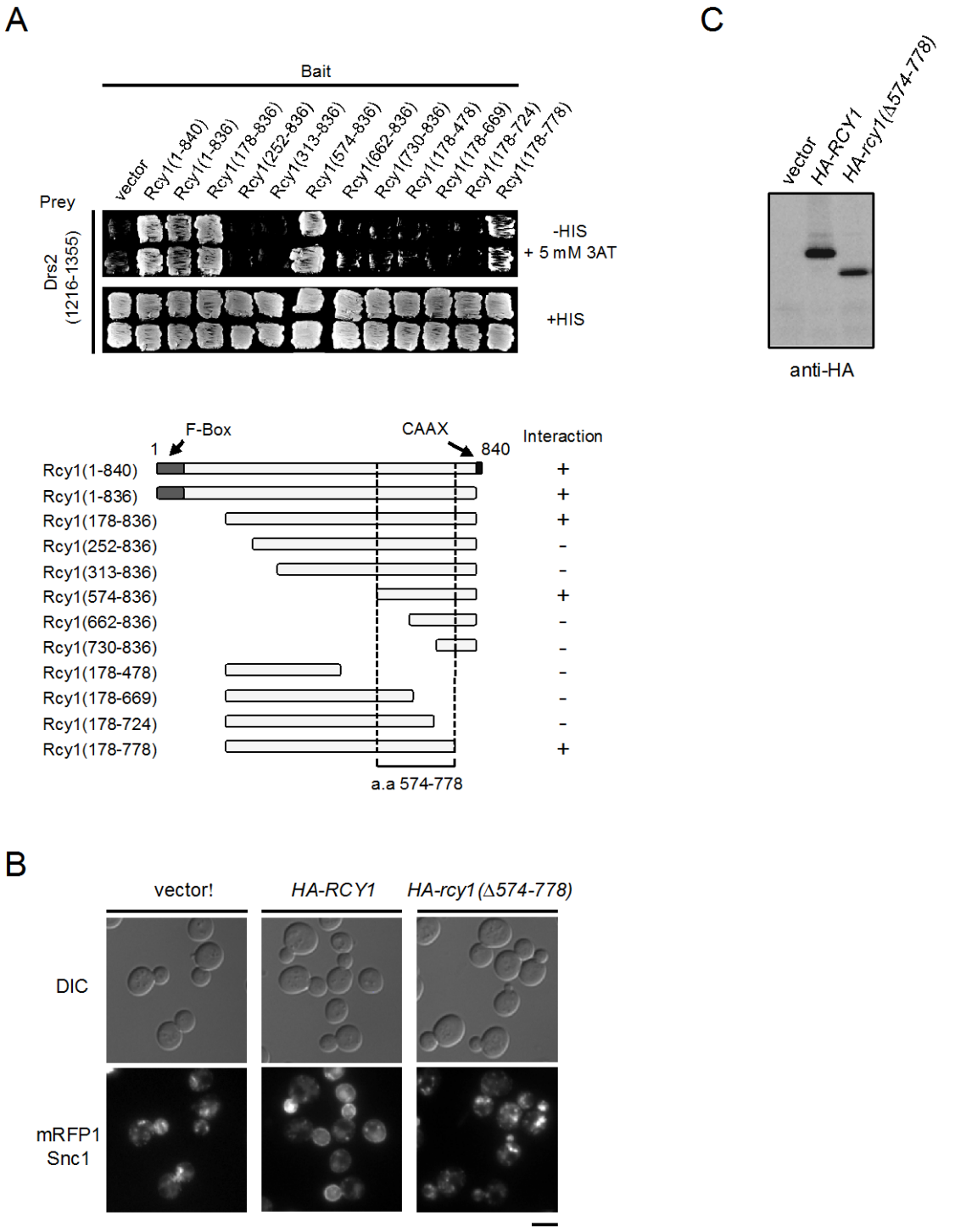
A
Bait
vector
Rcy1(1-840)
Rcy1(1-836)
Rcy1(178-836)
Rcy1(252-836)
Rcy1(313-836)
Rcy1(574-836)
Rcy1(662-836)
Rcy1(730-836)
Rcy1(178-478)
Rcy1(178-669)
Rcy1(178-724)
Rcy1(178-778)
Prey
Drs2
(1216-1355)
-HIS
+ 5 mM 3AT
+HIS
F-Box
CAAX
1
840
Interaction
Rcy1(1-840) +
Rcy1(1-836) +
Rcy1(178-836) +
Rcy1(252-836) -
Rcy1(313-836) -
Rcy1(574-836) +
Rcy1(662-836) -
Rcy1(730-836) -
Rcy1(178-478) -
Rcy1(178-669) -
Rcy1(178-724) -
Rcy1(178-778) +
a.a 574-778
C
vector
HA-RCY1
HA-rcy1(Δ574-778)
anti-HA
B
vector!
HA-RCY1
HA-rcy1(Δ574-778)
DIC
mRFP1
Snc1

Fig. 4 The Drs2p-interacting region of Rcy1p is functionally important.

(A) Drs2p(1216-1355) interacts with a C-terminal region of Rcy1p. Two-hybrid interaction was examined as in **Fig. 3A** using L40 carrying the *DRS2(1216-1355)* prey plasmid (pKT1865) and various deletion mutants of *RCY1* in bait plasmids (pKT1652, pKT1734, pKT2034-2043). The results are schematically summarized below. Expression of Rcy1p deletion proteins was confirmed by western blotting (data not shown). (B) Endocytic recycling of mRFP1-Snc1p in the *rcy1(Δ574-778)* mutant. YKT1780 (*rcy1Δ mRFP1-SNC1*) was transformed with YEplac195, YEplac195-*3HA-RCY1* (pKT1626), and YEplac195-*3HA-RCY1(Δ574-778)* (pKT2053). The transformant cells were grown to mid-logarithmic phase at 30°C, followed by microscopic observation using differential interference contrast (DIC) and GFP fluorescent (mRFP1-Snc1) optics. Bar, 5 μm. (C) Expression of Rcy1p(Δ574-778). YKT951 (*rcy1Δ*) was transformed with YEplac195, YEplac195-*3HA-RCY1*, and YEplac195-*3HA-RCY1(Δ574-778)*. Protein expression was confirmed by Western blotting using an anti-HA antibody.

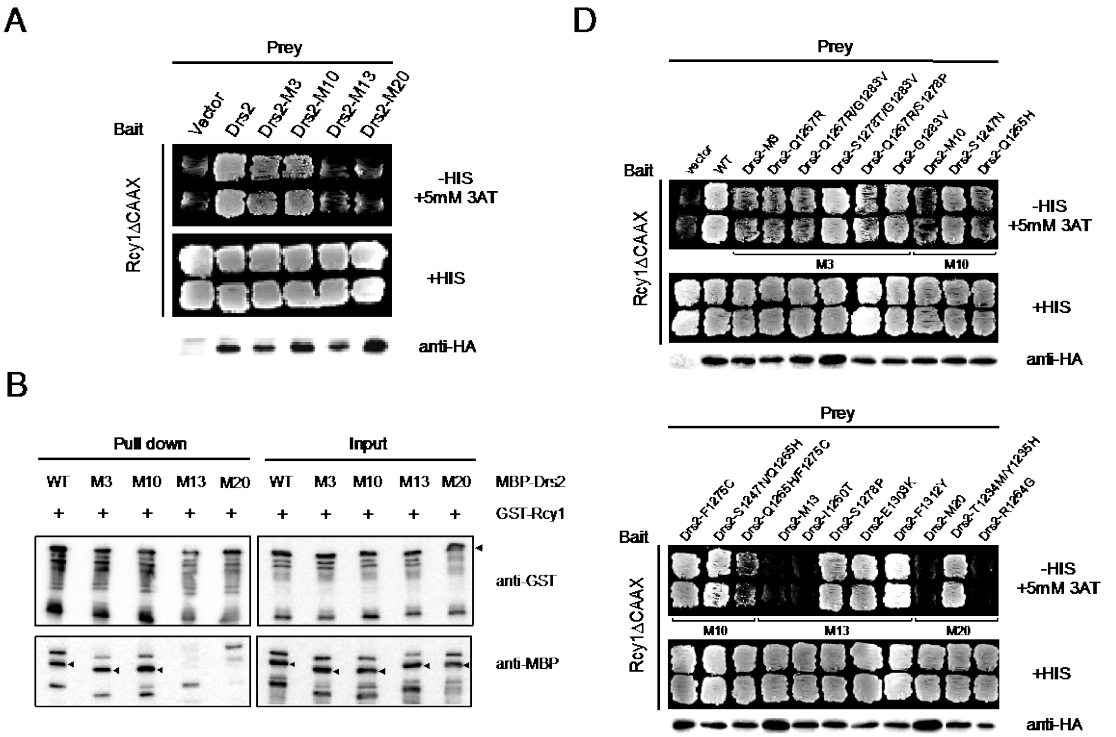

Drs2 mutant	Interaction	Drs2 mutant	Interaction
vector	-	**Drs2-M13**	-
Drs2-C (WT)	++	L1217P	NT
Drs2-M3	+	D1220H	NT
Q1267R	+	I1260T	-
Q1267R/G1283V	+	S1278P	++
S1278T/G1283V	++	E1303K	++
Q1267R/S1278P	+	F1312Y	++
G1283V	++	**Drs2-M20**	-
Drs2-M10	+	T1234M/Y1235H	++
S1247N	++	R1264G	-
Q1265H	+		
F1275C	++		
S1247N/Q1265H	++		
Q1265H/F1275C	+		

NT : Not Tested

Fig. 5 Identification of amino acid residues in the Drs2p C-terminal region that are required for the interaction with Rcy1p.

(A) Isolation of *drs2* mutants that fail to interact with Rcy1p in two-hybrid. YHH22 carrying *RCY1*Δ*CAAX* (pKT1652) was transformed with prey plasmids (pKT1866-1869) containing the indicated mutations in Drs2p(1216-1355), and the transformants were grown as in **Fig. 3A**. Mutant protein expression was confirmed by western blotting using an anti-HA antibody. (B) Interaction of Drs2p mutants with Rcy1p in pull-down assay. Experiments were carried out as described in **Fig. 3B**. (C) Amino acid substitutions identified in each mutant. Amino acid substitutions that impair the interaction with Rcy1p are indicated with boldface. (D) Identification of amino acid residues in the Drs2p C-terminal region that are required for the interaction with Rcy1p. YHH22 carrying *RCY1*Δ*CAAX* (pKT1652) was transformed with prey plasmids containing the indicated mutations, which were introduced by site-directed mutagenesis. The transformants were grown as in **Fig. 3A**. Expression of each mutant protein was verified by western blotting. The results are summarized with relative strength of the interaction from wild-type (++) to no interaction (-). In the analyses of Drs2-M3, Q1267R/S1278P was constructed instead of Q1267R/S1278T because the mutation primer for S1278P was available from the analyses of Drs2-M13.

A

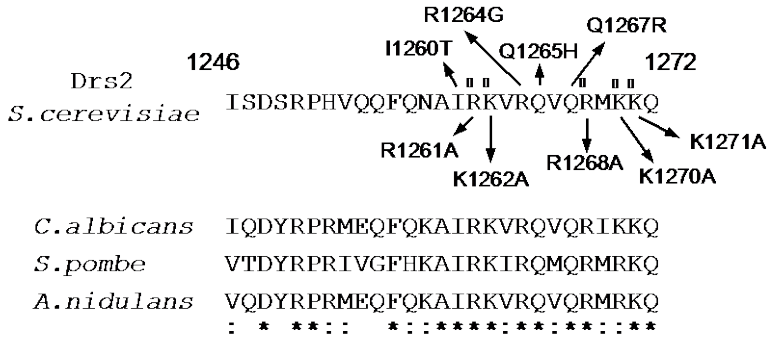
R1264G
Q1267R
I1260T
Q1265H
1246
1272
Drs2
S.cerevisiae
ISDSRPHVQQFQNAIRKVRQVQRMKKQ
R1261A
K1262A
R1268A
K1270A
K1271A
C.albicans IQDYRPRMEQFQKAIRKVRQVQRIKKQ
S.pombe VTDYRPRIVGFHKAIRKIRQMQRMRKQ
A.nidulans VQDYRPRMEQFQKAIRKVRQVQRMRKQ

B

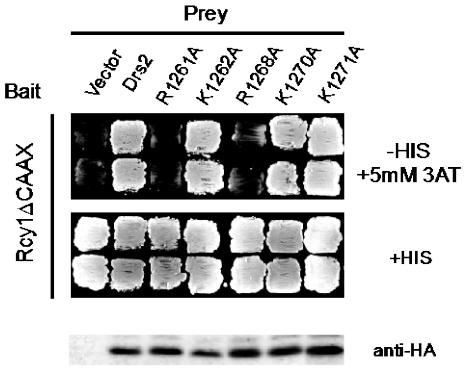
Prey
Bait
Vector
Drs2
R1261A
K1262A
R1268A
K1270A
K1271A
Rcy1ΔCAAX
-HIS
+5mM 3AT
+HIS
anti-HA

C

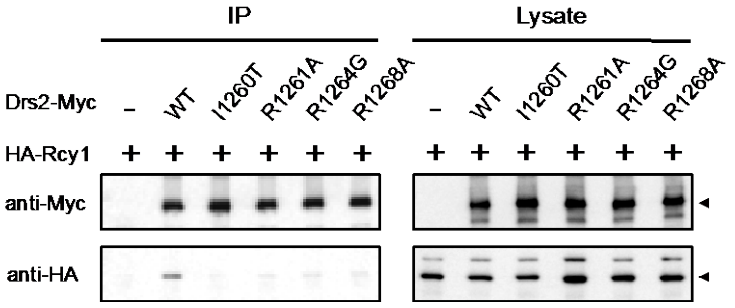
IP
Lysate
Drs2-Myc
HA-Rcy1
anti-Myc
anti-HA
–
WT
I1260T
R1261A
R1264G
R1268A
+

Fig. 6 Further mutational analysis of the Rcy1p-interacting region of Drs2p.

(A) Multiple sequence alignment of Drs2p (amino acids 1246-1272) and its homologues in fungi. The ClustalW algorithm was used to create the alignment. Black diamonds indicate conserved basic residues that were mutated to alanine. Asterisks and colons indicate identical and similar amino acids, respectively. Database accession numbers are: *S. cerevisiae* (P39524), *C. albicans* (Q5ADR3), *S. pombe* (O94296), and *A. nidulans* (Q5B018). (B) Two-hybrid interaction of mutant Drs2-C proteins. YHH22 carrying *RCY1ΔCAAX* (pKT1652) was transformed with prey plasmids (pKT1909-1913) containing the indicated mutations in Drs2p(1216-1355), and the transformants were grown as in **Fig. 3A**. Mutant protein expression was confirmed by western blotting using an anti-HA antibody. (C) Coimmunoprecipitation of HA-Rcy1p with Drs2 mutant proteins. A wild-type strain (YKT38) carrying *HA-RCY1* on a multicopy plasmid (pKT1626) was transformed with a centromeric plasmid containing the wild-type *DRS2* (pKT1860), *drs2-I1260T* (pKT1883), *drs2-R1261A* (pKT1914), *drs2-R1264G* (pKT1884) or *drs2-R1268A* (pKT1916). Myc-tagged Drs2 proteins were immunoprecipitated (IP) with an anti-Myc antibody from the membrane protein extracts, and the immunoprecipitates were analyzed by western blotting using anti-Myc and -HA antibodies. The membrane protein extracts prior to immunoprecipitation (Lysate) were also analyzed by western blotting.

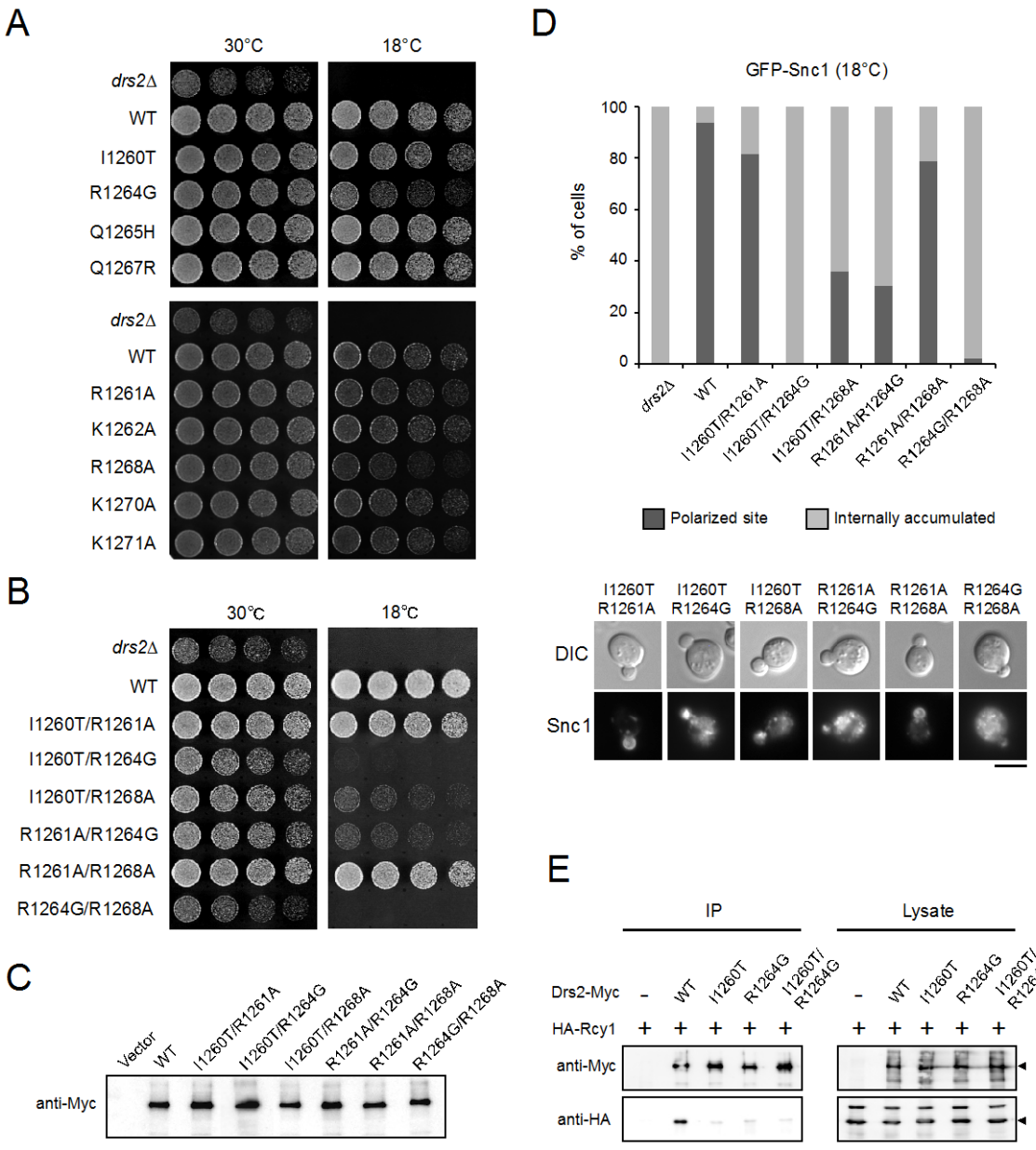
A
30°C
18°C
drs2Δ
WT
I1260T
R1264G
Q1265H
Q1267R
drs2Δ
WT
R1261A
K1262A
R1268A
K1270A
K1271A
B
30°C
18°C
drs2Δ
WT
I1260T/R1261A
I1260T/R1264G
I1260T/R1268A
R1261A/R1264G
R1261A/R1268A
R1264G/R1268A
C
Vector
WT
I1260T/R1261A
I1260T/R1264G
I1260T/R1268A
R1261A/R1264G
R1261A/R1268A
R1264G/R1268A
anti-Myc
D
GFP-Snc1 (18°C)
% of cells
100
80
60
40
20
0
drs2Δ
WT
I1260T/R1261A
I1260T/R1264G
I1260T/R1268A
R1261A/R1264G
R1261A/R1268A
R1264G/R1268A
Polarized site
Internally accumulated
I1260T R1261A
I1260T R1264G
I1260T R1268A
R1261A R1264G
R1261A R1268A
R1264G R1268A
DIC
Snc1
E
IP
Lysate
Drs2-Myc
HA-Rcy1
WT
I1260T
R1264G
I1260T/ R1264G
anti-Myc
anti-HA

Fig. 7 Functional analyses of *drs2* mutants that abolish the interaction with Rcy1p.

(A) Cold-sensitive growth of *drs2* mutants. Cells of a *drs2*Δ mutant (YKT746) carrying pKT1443 (*GFP-SNC1*) were transformed with a control vector or a centromeric plasmid containing the wild-type *DRS2* (pKT1860) or the indicated mutant (pKT1883-1884, pKT1906-1907, and pKT1914-1918). The transformant cells were serially diluted 2-fold, spotted onto YPDA plates, followed by incubation at 30°C and 18°C for 1 and 3 days, respectively. (B) Cold-sensitive growth of *drs2* mutants containing two amino acid substitutions. Cells of a *drs2*Δ mutant (YKT746) carrying pKT1443 (*GFP-SNC1*) were transformed with a control vector or a centromeric plasmid containing the wild-type *DRS2* (pKT1860) or the indicated mutant (pKT1908, pKT2055-2059). The transformant cells were grown as in (A), except that incubation time at 18°C was 4 days. (C) Expression of Drs2 mutant proteins. Protein expression was confirmed in cells of a wild-type (YKT38) strain transformed with the plasmids described in (B) by western blotting using an anti-Myc antibody. (D) Endocytic recycling of GFP-Snc1p in *drs2* mutants. The cells in (B) were grown to mid-logarithmic phase at 30°C or 18°C for 12h. The percentage of small-budded cells with polarized or intracellularly accumulated GFP-Snc1p was determined by microscopic examination (n > 100). Representative images of differential interference contrast (DIC) and GFP-Snc1p (Snc1) at 18°C are shown below. Bar, 5 μm. (E) Coimmunoprecipitation of HA-Rcy1p with Drs2p-I1260T/R1264G-Myc. Experiments were performed as in **Fig. 6C** with an additional strain containing pKT1908 (*drs2-I1260T/R1264G*).

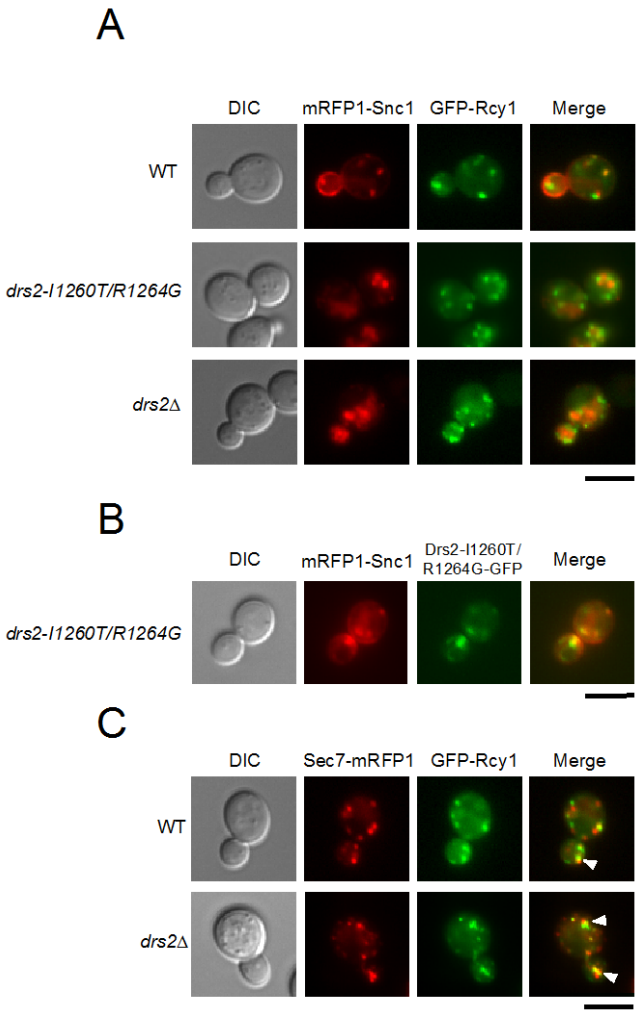
A
DIC
mRFP1-Snc1
GFP-Rcy1
Merge
WT
drs2-I1260T/R1264G
drs2Δ
B
DIC
mRFP1-Snc1
Drs2-I1260T/
R1264G-GFP
Merge
drs2-I1260T/R1264G
C
DIC
Sec7-mRFP1
GFP-Rcy1
Merge
WT
drs2Δ

Fig. 8 Rcy1p may be localized to early endosomes in a Drs2p-dependent manner.

(A) GFP-Rcy1p is not localized to mRFP1-Snc1p-containing membranes in *drs2-I1260T/R1264G and drs2*Δ mutants. Wild-type (YKT38) (WT) and *drs2*Δ (YKT746) (*drs2*Δ) strains carrying pRS416-*mRFP1-SNC1* (pKT1563) were transformed with YEplac181-*GFP-RCY1* (pKT1560), and the *drs2*Δ strain containing pKT1563 was also transformed with YEplac112-*GFP-RCY1* (pKT2054) and YCplac111-*DRS2-I1260T/R1264G* (pKT1908) (*drs2-I1260T/R1264G*). The transformants were grown to mid-logarithmic phase at 30°C in SD-Leu-Ura medium (WT, *drs2*Δ) or SD-Leu-Ura-Trp medium (*drs2-I1260T/R1264G*). (B) Drs2p-I1260T/R1264G-GFP is localized to mRFP1-Snc1p-containing membranes. The *drs2*Δ strain carrying *mRFP1-SNC1* in (A) was transformed with YCplac111-*DRS2-I1260T/R1264G-GFP* (pKT2104), and the transformant was grown in SD-Leu-Ura medium as in (A). (C) Colocalization of GFP-Rcy1p with Sec7p-mRFP1. *SEC7-mRFP1* (YKT905) and *drs2*Δ *SEC7-mRFP1* (YHH636) strains were transformed with pKT1560 (*GFP-RCY1*). The resulting transformants were grown to mid-logarithmic phase at 30°C in SD-Leu medium. Obtained images were merged to compare the two signal patterns. Arrowheads indicate colocalization between GFP-Rcy1p and Sec7p-mRFP1. Bars, 5 μm.

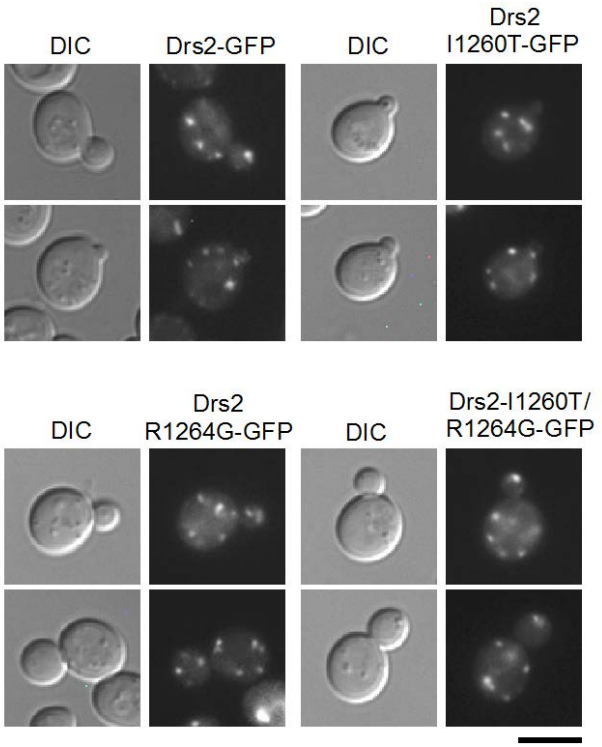

Fig. 9 Localization of Drs2 mutant proteins.

Wild-type strain (YKT38) was transformed with YCplac111-*DRS2-GFP* (pKT2123), YCplac111-*DRS2-I1260T-GFP* (pKT2124), YCplac111-*DRS2-R1264G-GFP* (pKT2125), and YCplac111-*DRS2-I1260T/R1264G-GFP* (pKT2104). The transformants were grown to mid-logarithmic phase at 30°C in SD-Leu medium. Differential interference contrast (DIC) and GFP (Drs2 R1264G-, I1260T-, I1260T /R1264G-GFP) images are shown. Bar, 5 μm.

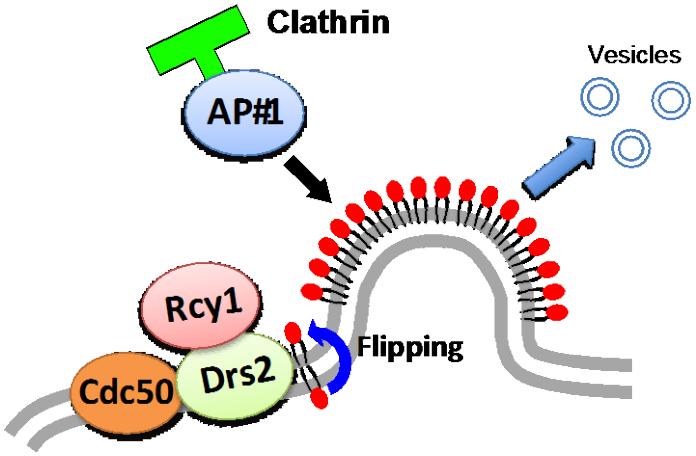

Fig. 10 A model for the function of Rcy1p in the Drs2p-mediated vesicle formation.

Rcy1p may spatiotemporally coordinate phospholipid flipping, cargo recruitment, and clathrin adaptor (e.g. AP-1) recruitment at the site where Drs2p is flipping phospholipids..